# Photoelectron diffraction effects in core-level photoemission from Na and Te atoms adsorbed on Ni(001)

N. V. Smith, H. H. Farrell, and M. M. Traum
*Bell Laboratories, Murray Hill, New Jersey 07974*

D. P. Woodruff, D. Norman,* M. S. Woolfson, and B. W. Holland
*Department of Physics, University of Warwick, Coventry CV4 7AL, United Kingdom*

(Received 28 September 1979)

The diffraction of photoelectrons emitted from the Na 2*p* and Te 4*d* core levels has been investigated both experimentally and theoretically for these atoms adsorbed in various configurations on an Ni(001) surface. The experiments were performed in the photon energy range $\hbar\omega = 70$–$115$ eV and the various modes of observing the photoelectron diffraction effects are described. Emphasis is on the azimuthal diffraction patterns which are shown to be sensitive to photoelectron kinetic energy, polar angle of emission, and adsorbate species. It is found that these patterns can be matched quite well by theoretical calculations using a multiple-scattering formalism and parameters taken from previous low-energy electron diffraction studies. In the case of Na, no adjustment is required to these parameters. In the case of Te, a match is obtained only after a rigid shift of the energy scale by 8 eV. The sensitivity of the calculated diffractions patterns to the input parameters is reported, and it is suggested that the measurements could form the basis of a surface structural technique with a $d_\perp$ spacing sensitivity of $\sim 0.1$ Å.

## I. INTRODUCTION

The anisotropy of photoemission from core levels is of interest for two main reasons. The first is purely theoretical. Core levels are highly localized, so that photoemission from core levels on different atoms can be treated incoherently. Since a fully first-principles theory of photoemission has proved difficult to apply, this appealing simplification should be useful in devising experimental tests and further development of the theory. This first reason has been overshadowed in much recent discussion by a second, and more practical, reason. If it is indeed possible to observe and to understand the anisotropies in photoemission from core levels of *adsorbed atoms on surfaces*, this could form the basis of a new technique for the determination of the atomic structure of surfaces.[1,2]

The experiments described in this paper were undertaken as part of a program whose objectives were: (a) to detect the anisotropies in core-level photoemission, (b) to determine the magnitudes and general phenomenology of these anisotropies, (c) to perform theoretical calculations and compare with the observed anisotropies, and (d) to assess the prospects for a new surface structural technique based on the observed effects. As will be seen, each of these objectives was achieved to some degree.

We shall be concerned with the angular dependence of photoemission from core levels of adsorbed atoms. The essential physics is illustrated schematically in Fig. 1. Following Liebsch,[1] the wave function of the emitted photoelectron is represented in two parts,

$$\Psi = \Psi^0 + \Psi^1 . \tag{1}$$

The first term $\Psi^0$ represents a wave propagating directly towards the detector. The second term $\Psi^1$ represents the composite of all the waves produced by single- and multiple-scattering processes against neighboring atoms. It is the interference between these waves which should give rise to observable diffraction effects. The proposed surface structural technique based on this effect has been dubbed photoelectron diffraction (or PhD).

There are a number of possible ways in which one might propose to observe PhD. One way would be to keep the analyzer and sample fixed, and then sweep the photon energy $\hbar\omega$. This varies the photoelectron wavelength, and the resulting spectrum would be analogous to an *I-V* characteristic in the closely related and well-established technique of low-energy-electron diffraction (LEED). Alterna-

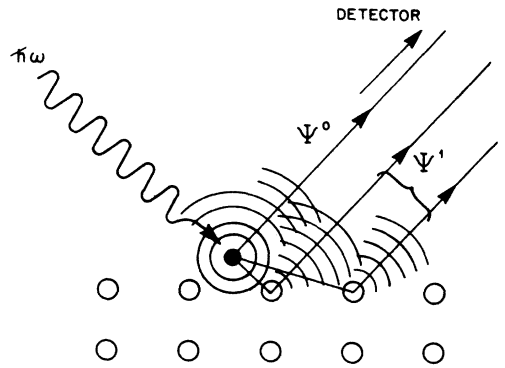


FIG. 1. Schematic representation of the emission of a photoelectron from an adsorbate atom core level.

 

tive methods involve varying the polar or azimuthal angles of emission. We have concentrated largely on the azimuthal dependence. This was done by keeping the analyzer fixed and rotating the sample about its surface normal. It will be readily appreciated that, if the surface were a uniform plane, no variations in intensity would be observed. Any variations seen can therefore be due only to atomic structure in the surface, and it is this consideration which has led us to favor the azimuthal dependence.[3] Other modes of measurement have been tried and will also be discussed.

Irrespective of which measurement mode is chosen, it is desirable to be able to tune $\hbar\omega$ so that the kinetic energies $E$ of the photoelectrons fall in the range 30–200 eV appropriate to LEED. Synchrotron radiation is therefore required. The advantage of working in this energy range is that the considerable expertise accumulated in LEED theory can be applied directly to the photoemission problem. If PhD does ultimately prove to be a useful surface structual tool, it has two potential advantages over LEED. First, the adsorbate overlayer does not need to be periodic as in LEED. Second, because of the energy selectivity of photoemission, one can tune in on core levels specific to the adsorbed atoms. Since the signal is then originating entirely from the atoms whose position one is trying to determine, the information content of the data should be quite high. If, on the other hand, the main usefulness of PhD is in testing and extending the fundamental theory of photoemission, it would still be desirable to work in the LEED energy range, because the current photoemission theories[1,2] lean very heavily on the theory of LEED.

The organization of this paper is as follows. Experimental methods are described in Sec. II. The results are then presented in two parts: Sec. III is concerned with the various ways in which photoelectron diffraction can be observed; Sec. IV, on the other hand, focuses on one particular mode of observation, the azimuthal dependence, and compares the results obtained in this mode for a variety of sample conditions. The theoretical calculations are described in Sec. V. In Sec. V and in Sec. VI, the prospects for using PhD in real surface structural studies will be assessed. Preliminary accounts of some aspects of this work have already been presented elsewhere.[4]

## II. EXPERIMENTAL METHODS

### A. Light source

The light source used in these experiments was the Tantalus storage ring located at the University of Wisconsin Synchrotron Radiation Center. Monochromatic radiation was produced by means of a Miyake-type plane-grating grazing-incidence monochromator,[5] which provided usable photon flux in the approximate range 60–150 eV. The binding energies relative to the Fermi level $E_F$ of the core levels examined, Na $2p$ and Te $4d$, are approximately 31 and 41 eV, respectively, so that the photoelectron kinetic energies fall nicely in the LEED energy range described in the Introduction. The ultimate resolution of the monochromator, determined by the size of the synchrotron radiation source, is ~0.7 Å. This, however, is not adequate to separate the spin-orbit-split components of all the core levels studied, and it was found convenient to widen the exit slit and use the poorer bandpass of 2.5 Å for most of the work. This ensures integration over the spin-split levels. The resolution of the electron energy analyzer was likewise degraded so as to take advantage of the resulting higher signal levels.

### B. Measurement system

The experimental chamber used in these studies is an angle-resolving photoemission system used in earlier studies[3,6] and modified to permit medium-energy-electron diffraction (MEED) characterization of the surface overlayer structure. The geometry is shown in Fig. 2. The radiation is incident upon the sample at an angle $\theta_i = 45°$ with respect to the surface normal and is $p$ polarized. An analyzer of the plane-mirror variety[6] can accept photoelectrons over a range of polar angles $\theta$ in the plane of incidence. The azimuthal angle $\phi$ can be varied through the entire 360° by rotating the sample about its surface normal. The sample is retractable to a second position (as shown) where it is illuminated at grazing incidence by an electron beam (energy ~4.5 keV) to perform the MEED characterization. While not as satisfactory as LEED, the MEED procedure was found to be adequate in determining good surface order and in distinguishing the $p(2\times2)$ and $c(2\times2)$ configurations.

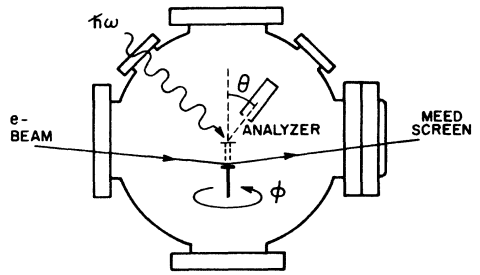


FIG. 2. Geometry of the experimental chamber defining the angular variables and showing the two alternative positions of the sample.

### C. Sample preparation

The Ni(001) samples were prepared by standard techniques and were cleaned *in situ* by argon ion bombardment and annealing. The surface condition was monitored by MEED as described above. The Na and Te overlayers were produced by direct evaporation from solid sources. The Na was obtained by resistive heating of commercially available channels. The Te was obtained by heating of solid pellets of Te contained within pyrex tubes according to the procedure described by Hagstrum and Becker.[7]

### D. Data manipulation

The core-level peaks in the photoemission energy spectra are superimposed on a background, sometimes of comparable intensity, due to the inelastic scattering of more energetic photoelectrons. Provision was made for removing this background. This was done usually by measuring the counting rate at an electron kinetic energy 5–7 eV higher than the core-level peak and then subtracting this from the counting rate measured at the peak itself. Since the inelastic background generally decreases with increasing kinetic energy, our method tends to be a slight underestimate of the true background.

There is the interesting question of whether the background is itself significantly anisotropic. This is clearly important if the anisotropies in the superimposed core-level emission are weak. This is discussed in Sec. III.

Much of our effort concentrated on the azimuthal dependence. An example of a set of azimuthal data taken for the Te 4*d* level on Ni(001)$p(2\times2)$Te is shown in the radial plot of Fig. 3. The open circles are the raw data after subtraction of the background as described above. The data were obtained point by point and were taken over all four quadrants. The full points represent the data after fourfold averaging (i.e., after combining measurements for $\phi$ values separated by $n\pi/2$ where $n$ is an integer) and are repeated in each quadrant. Note that this procedure does not introduce the mirror symmetry about the ⟨110⟩ and ⟨100⟩ azimuths. The observation that the measurements display this symmetry provides a valuable check on the internal consistency of the data. The outer full curve in Fig. 3 has been drawn smoothly through data to which mirror averaging has been applied. This therefore takes full advantage of the surface symmetry in enhancing the statistics. The accumulated number of counts in a typical averaged measurement is generally $\gtrsim10^4$, so that the purely statistical noise is at the ~1% level. The inner full curve of Fig. 3 represents the same information as the outer curve, but has had a further "background" removed by subtraction of the minimum value. This can be a rather misleading way of presenting the data since it overdramatizes the azimuthal variations. It is quite commonly used, however (sometimes with, and sometimes without, the mirror-symmetrizing step), and is of value in displaying the way in which the azimuthal anisotropies vary with other parameters such as $\theta$ and $E$. In this paper we shall be employing these various methods of data display as well as linear plots of photoemission intensity versus $\phi$.

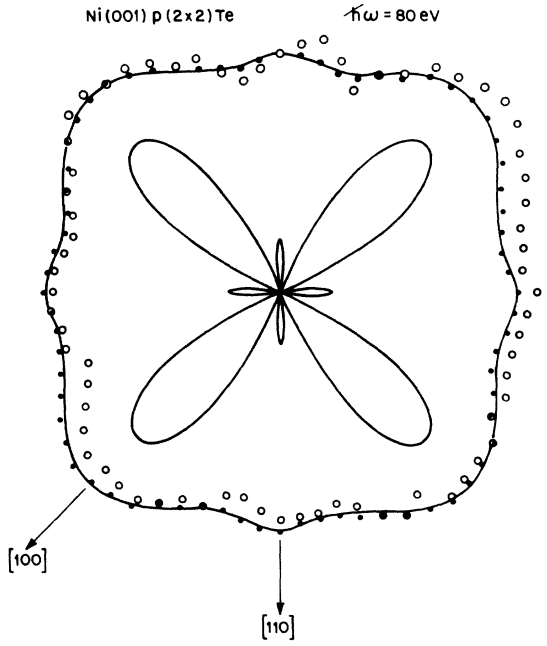


FIG. 3. Radial plot of the azimuthal dependence of the Te 4*d* emission from Ni(001)$p(2\times2)$Te. The open circles represent the raw data after subtraction of the inelastic background under the core-level peak; the full circles are a fourfold-averaged version of the same data; the outer full curve has been drawn smoothly through the data points after averaging points equivalent by mirror symmetry; the inner full curve is obtained from the outer full curve by subtraction of a minimum value and multiplication by 5. This is intended to illustrate the manipulations which have been used to enhance the statistics of the data and eliminate spurious variations.

## III. GENERAL RESULTS

One of the aims of this program was to survey the phenomenology of PhD, and some of the more general aspects of the data are described in this section.

### A. Adsorbate effect on substrate emission

The presence of an adsorbate overlayer affects the emission from the substrate. Figure 4 com-

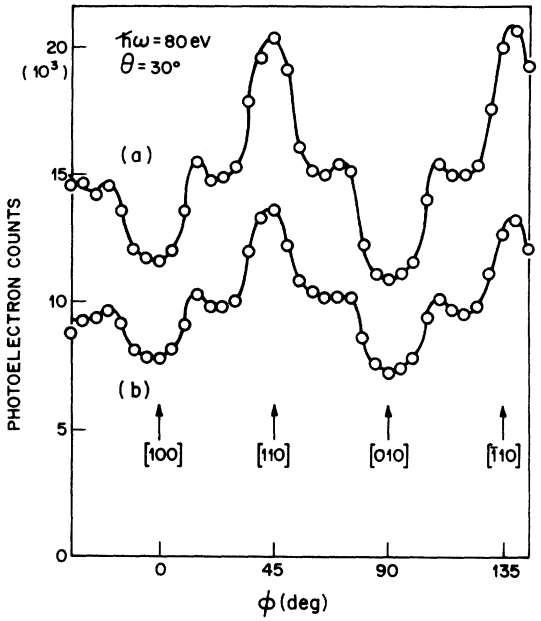


FIG. 4. Azimuthal dependence of the Ni 3*d* emission from: (a) clean Ni(001), (b) the same surface with a $c(2\times 2)$ overlayer of Na.

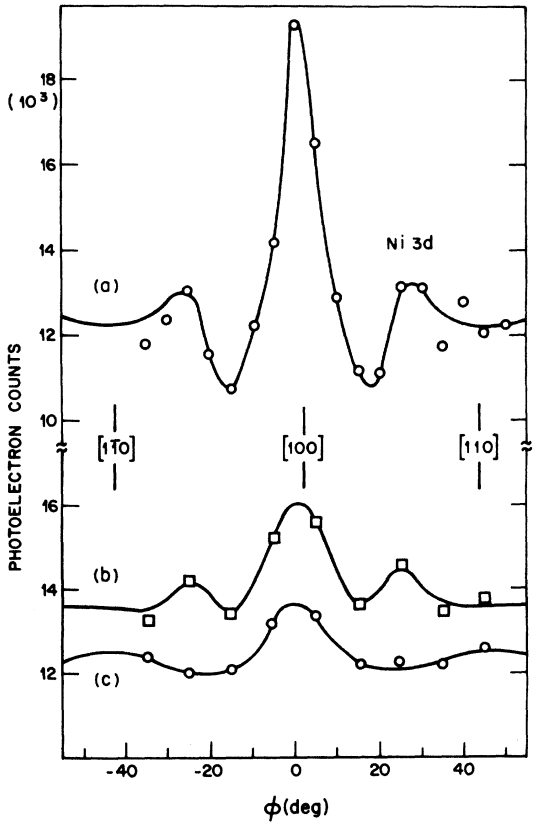


FIG. 5. Comparison of the azimuthal dependence of: (a) the Ni 3*d* emission from Ni(001) with the emission at two kinetic energies within the inelastic tail, (b) $E = 85$ eV, (c) $E = 55$ eV. The photon energy has $\hbar\omega = 100$ eV corresponding to a mean Ni 3*d* kinetic energy $E \sim 93$ eV. The energy band width of the analyzer was large enough to integrate over the whole Ni 3*d* valence band.

pares the azimuthal dependence of the Ni 3*d* valence emission from clean Ni(001) with that obtained from Ni(001)$c$ $(2\times 2)$Na. In these measurements the energy window of the electron energy analyzer was wide enough to integrate over the entire 3*d* band. The data were taken at $\theta = 30°$ and $\hbar\omega = 80$ eV. In both cases the azimuthal anisotropy is seen to be quite strong. The effect of Na adsorption is to attenuate the Ni 3*d* emission; the actual shape of the azimuthal dependence is unaltered. This insensitivity of the azimuthal diffraction pattern to adsorption indicates that measurements of the substrate emission are highly unlikely to yield surface structural information. A similar conclusion has been arrived at earlier in the study of adsorbate effects on the angular dependence of substrate Auger emission.[8]

### B. Background anisotropies

It was found in these studies that the background of inelastically scattered electrons for clean Ni surfaces displayed measurable anisotropy. While this is of obvious importance in the background subtraction procedure described in Sec. II D, the results are of physical interest in their own right. Figure 5 shows results for the azimuthal dependence of photoemission from clean Ni(001) at $\theta = 55°$ and $\hbar\omega = 100$ eV. The photoemission from the Ni 3*d* valence bands is seen to be markedly anisotropic. Also shown in Fig. 5 are the azimuthal plots obtained at various energies in the inelastic background arising from the Ni 3*d* emission. These show appreciable anisotropies which resemble, in attenuated form, the anisotropy of the Ni 3*d* emission itself. These observations are typical of those taken over a range of values of $\theta$ and $E$.

Observations such as those in Fig. 5 permit us to distinguish between two contributing effects to the anisotropy. One contribution to the anisotropy would arise through diffraction effects as the electron propagates through the crystal after scattering. One would expect, however, that such effects would depend on the energy to which the electron has been scattered. The other contribution to the anisotropy would be a memory of the anisotropy in the primary excitation process. The resemblance of the azimuthal plots for inelastically scattered electrons and the primary Ni 3*d* emission evidently favors the latter contribution.

For high-energy electrons, the dominant decay mechanism is by plasmon emission and is strongly in the forward direction.[9] Anisotropy memory effects would therefore be expected. There is rea-

son to suppose that forward scattering would predominate in the lower-energy regions as well. In the basic theory of the simple interacting electron gas,[10] the imaginary part $\Gamma$ of the self-energy (inverse lifetime) of an electron of momentum $p$ is given by

$$\Gamma(p)=\frac{e^2}{2\pi^2}\int d^3q\,\frac{1}{q^2}\,\mathrm{Im}\left|\frac{1}{\epsilon(q,\omega)}\right| . \qquad (2)$$

The integral is over all processes in which the electron at energy $E$ $(=p^2)$ decays inelastically to energy $E-\omega$ with momentum transfer $\vec{q}$. The integral over $\vec{q}$ is restricted to those points for which $\vec{p}+\vec{q}$ lies between the spheres of radii $\sqrt{E}$ and $\sqrt{E-\omega}$. The alternative decay modes plasmon emission and particle-hole pair creation are contained in the loss function $\mathrm{Im}\left|\epsilon^{-1}(q,\omega)\right|$. The factor $q^{-2}$ in the integrand favors (after consideration of the limits of integration mentioned above) small momentum transfers and, thereby, forward scattering. Ni is, of course, a $d$-band metal rather than a simple free-electron gas, but one might expect similar considerations to apply. We propose that these considerations account qualitatively for the observed memory effects, and it would be desirable to investigate this further by performing detailed calculations using the theory from which Eq. (2) is derived.

### C. Polar-angle dependence

Some results for the polar-angle anistropy of core-level photoemission are shown in Fig. 6. Measurements were taken at $\hbar\omega=100$ eV for Na $2p$ levels in the system Ni(001)$c(2\times2)$Na and are compared with measurements taken at the same photon energy on the Ni $3d$ emission from clean Ni. (In the latter case, the energy resolution was such as to integrate over the entire Ni $3d$ valence band.) It is seen that the Ni $3d$ emission is quite anisotropic, indicating strong PhD effects. By contrast, the Na $2p$ emission is less anisotropic and consists of weak structures superimposed on a smoothly varying background.

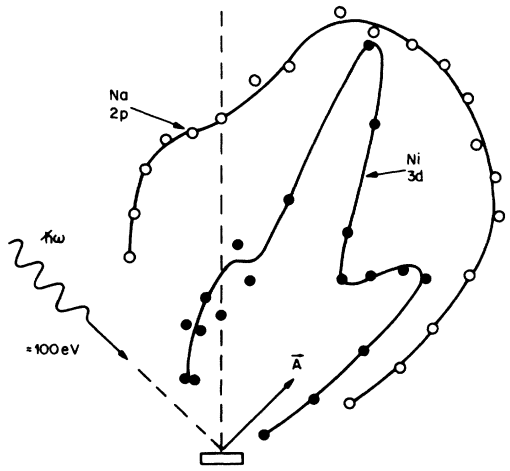


FIG. 6. Polar-angle dependence of the Na $2p$ emission from Ni(001)$c(2\times2)$Na compared with the Ni $3d$ emission from clean Ni(001). Smooth curves are drawn as a guide to the eye.

One disadvantage, for our present purposes, of measurements of the polar-angle dependence is that one is varying the angle between the direction of electron collection and the electromagnetic vector potential $\vec{A}$. The results, therefore, contain unwanted atomic effects[11] in addition to the desired PhD effects. There are also polar-angle variations due to refraction and escape considerations. These, as well as the inherent weakness of the diffraction structures, militate against the use of the polar plots as a means of obtaining quantitative surface structural information.

### D. CIS mode

One mode of observing PhD involves the use of constant-initial-state (CIS) spectroscopy. The essence of the method is to monitor the intensity of a core-level peak at one particular angle as $\hbar\omega$ is swept continuously. The technique therefore exploits the special continuum nature of synchrotron radiation. The PhD effects appear as oscillations in the $\hbar\omega$ dependence, and so the method bears a close resemblance to intensity analysis of $I$-$V$ characteristics in LEED. The method has been explored extensively by other groups,[12,13] and will therefore be treated only briefly here.

Measurements of the $\hbar\omega$ dependence of the Na $2p$ intensity in normal emission from Ni(001)$c(2\times2)$Na are shown as curve (a) in Fig. 7 in the range $\hbar\omega=70$–$115$ eV. The results are compared with the theoretical calculations for this system by Li and Tong,[14] and it is seen that there are no particularly strong correspondences in the energy locations of structure. The same sort of measurements have been reported by Williams *et al.* over a wider $\hbar\omega$ range and some correspondences are observed.[13] The data shown here are over a rather small energy range, and the useful part of this range is reduced further by the $M_{2,3}VV$ Auger emission which occurs over the energy interval indicated in Fig. 7. The data of curve (a) in Fig. 7 are not normalized to monochromator transmission, and the main broad maximum near $\hbar\omega=85$ eV occurs close to (but not at) the maximun in the monochromator throughput. For comparison we show as curve (b) in Fig. 7 the unnormalized total photoelectric yield from clean Ni(001); this contains structures characteristic of the total absorption cross section just above the Ni $3p$ edge. Our conclusion is that in cases such as the one here, when the PhD features

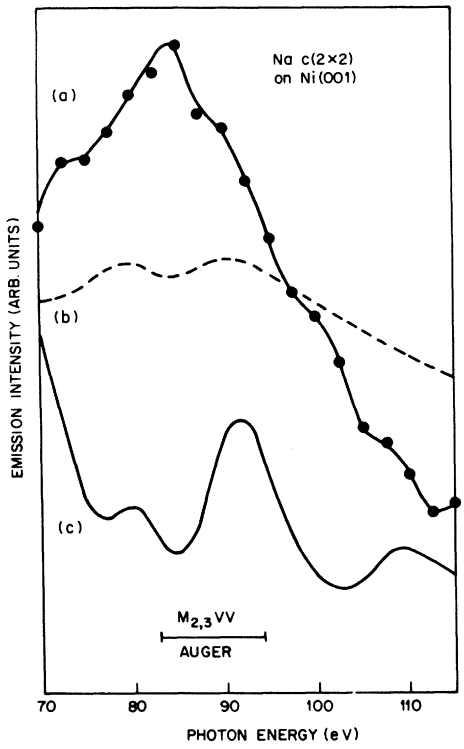


FIG. 7. Curve (a) is the measured normal CIS spectrum for Na $2p$ emission from Ni(001)$c(2\times2)$Na which has not been normalized to monochromator transmission; curve (b) is the total photoelectric yield from clean Ni (001), again uncorrected for monochromator transmission; curve (c) is a theoretically calculated normal CIS spectrum (Ref. 14).

are very weak compared with extraneous structures due to monochromator transmission, substrate absorption, etc., considerable caution should be applied in the comparison with theory. We do not present here any CIS data for Te adsorption. These are complicated by yet another effect, namely, the occurrence of a Cooper minimum in the atomic Te $4d$ cross section[15] whose effect is to dominate the gross shape of the CIS.

## IV. DETAILED AZIMUTHAL RESULTS

Our principal experimental approach in these studies has been the measurement of the azimuthal dependence of the core-level emission. This was performed by rotation of the sample about its surface normal, keeping the analyzer fixed in position. As stated above and elsewhere,[3] this approach has the advantage of isolating the PhD effects and is therefore immune from the complications discussed in the preceding section. It also provides valuable integrity checks on the data through crystal symmetry. We describe here some specific studies done with this approach.

### A. Energy dependence

Azimuthal plots taken at various photon energies are shown in Fig. 8 for Na $2p$ and Te $4d$ (binding energies 31 and 41 eV relative to $E_F$, respectively) for these atoms adsorbed in the $c(2\times2)$ configuration on Ni(001). The data points represent the result of an averaging procedure of data taken over two or more quadrants as described in Sec. II D. The full curves have been drawn smoothly through a mirror-averaged set.

The azimuthal variations are seen to be quite strong, and their precise form depends on the photon energy. For example, in the case of Na $2p$, the maximum emission at $\hbar\omega = 80$ eV coincides with the $\langle 100\rangle$ azimuths. At $\hbar\omega = 90$ eV, the maximum is weaker and occurs along the $\langle 110\rangle$ azimuths; it then reverts to the $\langle 100\rangle$ azimuths at $\hbar\omega = 100$ eV. Qualitatively speaking, the changes with $\hbar\omega$ are just what one would expect as a consequence of varying the photoelectron de Broglie wavelength. At $\hbar\omega = 80$, 90, and 100 eV, the respective values for the photoelectron kinetic energy $E$ are approximately 33, 43, and 53 eV in the case of Te $4d$, and 46, 56, and 66 eV in the case of Na $2p$. Note that we have taken into account the 2–3 eV lowering of the work function by adsorption of Na. The polar angle was kept at $\theta = 30°$ for all the data of Fig. 8, and so the corresponding values of the parallel wave vector for the photoelectron $k_{\parallel} = (2mE/\hbar^2)^{1/2}\sin\theta$ vary across the range 1.47–2.08 $\text{Å}^{-1}$.

Although Te and Na atoms on Ni(001) are believed to occupy the same coordination sites, it is seen that the azimuthal anisotropies are quite different. Note in this comparison that the value of $E$ is roughly the same for Na $2p$ at $\hbar\omega = 80$ (90) eV as it is for Te $4d$ at $\hbar\omega = 90$ (100) eV. The differences are attributed in part to differences in the $d_\perp$ spacing of the adsorbed atoms relative to the outermost Ni layer [2.23 Å in the case of Na (Ref. 16) and 1.90 Å in the case of Te (Ref. 17)]. Another source of difference lies in the intrinsic nature of the optical excitation event since the Na $2p$ states will couple to $l = 0$ and $l = 2$ components of the outgoing photoelectron wave, while Te $4d$ states will couple to $l = 1$ and $l = 3$ components.

The dashed curves in Fig. 8 represent the final results of extensive theoretical calculations and have been normalized to the experimental results at $\phi = \pm 20°$. The agreement is seen to be good both for the overall amplitudes of the PhD modulations and the reproduction of the shapes. It should be mentioned that to achieve this in the case of Te it was found necessary to allow the $\theta$ and $E$ values to deviate somewhat from their nominal experimental values. Detailed discussion and justification of

these calculations is deferred to Sec. V. The main point here is that the experimental azimuthal diffraction patterns have been shown to be theoretically consistent with the surface atomic structure as determined by LEED.

### B. Polar-angle dependence

The form of the azimuthal diffraction pattern depends on the polar angle $\theta$. This is illustrated in Fig. 9 which shows results for Te 4*d* emission from Ni(001)$c(2\times2)$Te at $\hbar\omega = 80$ eV. As in Fig. 8, the circles correspond to fourfold-averaged data and the smooth curves have been drawn through data which have also been mirror averaged.

The polar angles 30°, 45°, and 60° shown in Fig. 9 correspond to parallel wave vectors $k_{\parallel} = 1.47$, 2.08, and 2.55 Å$^{-1}$, respectively. The range of $k_{\parallel}$ is therefore somewhat larger than that obtained by varying $E$, as discussed in the preceding section. As far as one can tell at present, the qualitative changes obtained by varying $\theta$ differ from those obtained by varying $E$. If correct, this is a very encouraging result as far as surface structural determinations are concerned since it indicates that the $\theta$ dependence offers additional, rather than redundant, information.

As in the case of the $E$ dependence, the $\theta$ dependence of the azimuthal patterns can be well reproduced by the theoretical calculations, represented as dashed curves in Fig. 9. Details are to be found in Sec. V C.

### C. Configuration dependence

One of the claims that has been made for PhD as a surface structural technique is that the PhD diffraction patterns should be determined by the local coordination, and that long-range periodicity should not be important as it is in LEED. If true, this would mean that PhD could be used to study disordered and very low-coverage systems which are not accessible in LEED. One way to test this claim is to compare the PhD azimuthal patterns obtained for two different ordered coverages.

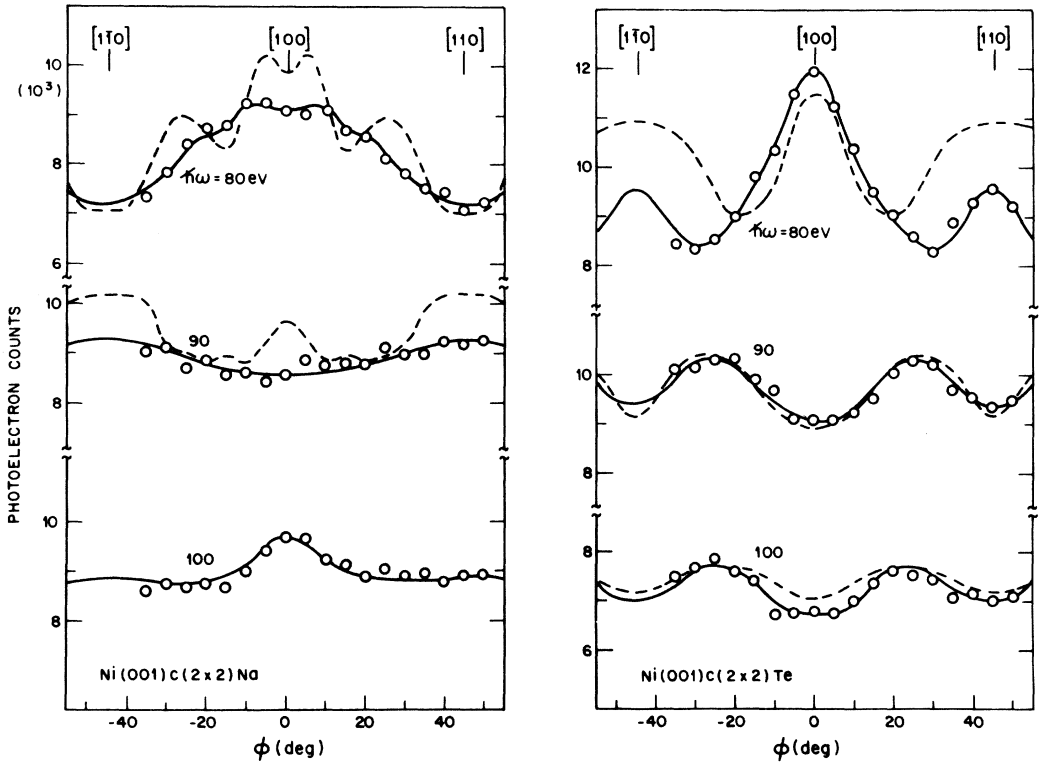


FIG. 8. Azimuthal dependence of adsorbate core-level photoemission at $\theta = 30°$ for the photon energies 80, 90, and 100 eV; results for Na 2*p*(Te 4*d*) are shown on the left (right). Open circles represent the fourfold-averaged experimental data; the full curves are drawn smoothly through a mirror-averaged version of the same data. The dashed curves represent the results of the theoretical calculations described in Sec. V, and have been normalized to the experimental curves at $\phi = \pm 20°$. In the case of Te these calculations apply to polar angles of 32°, 28°, and 28° for $\hbar\omega$ = 80, 90, and 100 eV, respectively, rather than the nominal experimental values. No theoretical curve is available for Na 2*p* at $\hbar\omega = 100$ eV because the calculations failed to converge reliably at this energy.

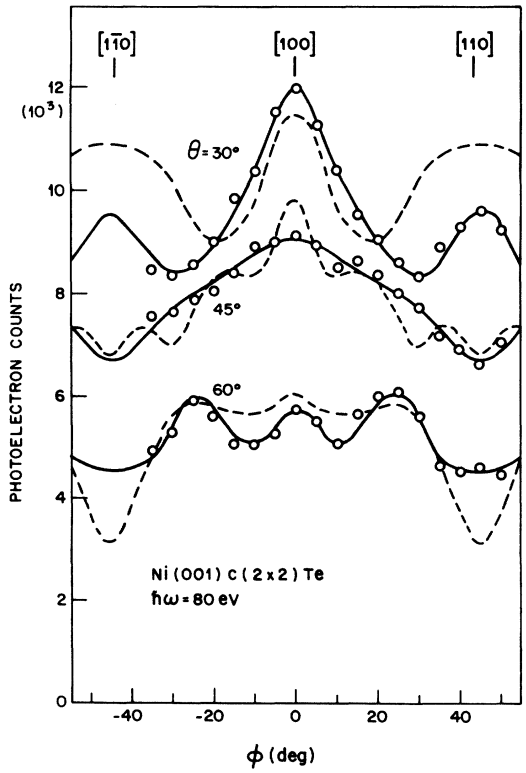


FIG. 9. Azimuthal dependence of the Te 4*d* emission from Ni(001)$c(2\times2)$ Te at $\hbar\omega = 80$ eV for various polar angles. The open circles and full curves represent the experimental data. The dashed curves represent theoretical results which apply to the polar angles 32°, 45°, and 58° rather than the nominal experimental values of 30°, 45°, and 60°.

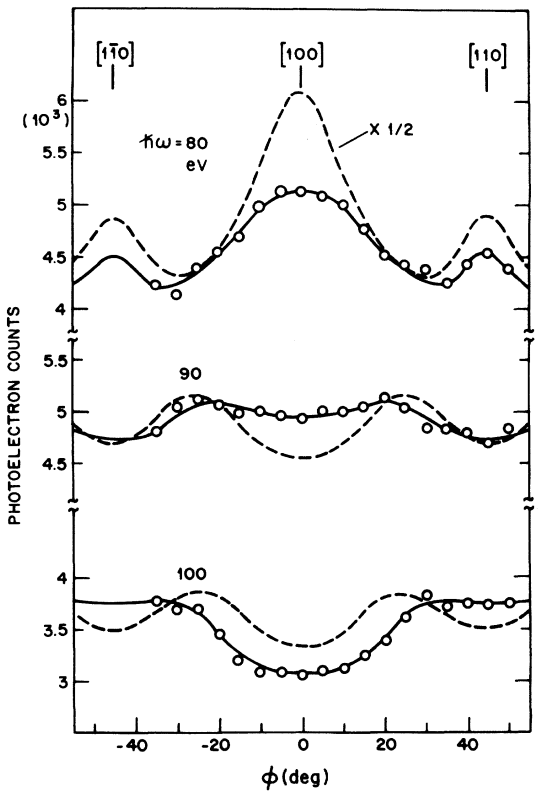


FIG. 10. Azimuthal dependence of Te 4*d* emission for Ni(001)$p(2\times2)$ Te represented by the open circles and full curves, compared with results for Ni(001)$c(2\times2)$Te represented by the dashed curves; the latter data is the same as that in Fig. 8 scaled down by a factor of $\frac{1}{2}$.

This has been done for Te on Ni(001), and Fig. 10 compares the results obtained for the $p(2\times2)$ and $c(2\times2)$ configurations.

The open circles and full curves in Fig. 10 represent the azimuthal diffraction patterns at $\hbar\omega = 80$, 90, and 100 eV for Ni(001)$p(2\times2)$Te. The dashed curves represent the corresponding patterns for Ni(001)$c(2\times2)$Te and are the same as in Fig. 8 except that they have been multiplied by $\frac{1}{2}$. The complete $c(2\times2)$ configuration has, of course, twice as many Te atoms as the $p(2\times2)$ configuration. If the experimental coverages were ideal and the diffraction patterns were determined only by local-site coordination, this normalization procedure would cause the two sets of data to coincide. It is seen in Fig. 10 that the magnitudes and gross shapes of the two sets of diffraction patterns are quite similar. The data are therefore in general support of the local-site coordination hypothesis.

Although the $p(2\times2)$ and $c(2\times2)$ diffraction patterns are grossly similar, there are some differences in detail. The structure in the $c(2\times2)$ data appears somewhat sharper. For example, the maximum at $\phi = 0°$ for $\hbar\omega = 80$ eV and the minima at $\phi = \pm 45°$ for $\hbar\omega = 100$ eV are noticeably better developed for the $c(2\times2)$ configuration. This could be attributed to scattering from an increased number of adsorbate neighbors or to secondary effects of long-range order. It was found in these experiments that the Te azimuthal diffraction patterns for both the $c(2\times2)$ and $p(2\times2)$ surfaces were slightly sharper after annealing the sample. This procedure also caused the MEED patterns to sharpen up, suggestive of improvement in the long-range periodicity. On the other hand, the sharpening of both the PhD and MEED patterns on annealing could indicate a greater occupancy by the adsorbate atoms of the equilibrium fourfold sites rather than nonequilibrium sites. This is a point which would be worthy of further study both experimentally and theoretically. From the theoretical point of view, it would be interesting to find out whether calculated azimuthal diffraction patterns for the $p(2\times2)$ are similar to those for the $c(2\times2)$ configuration.

## V. THEORETICAL CALCULATIONS

An important part of this project was to perform numerical calculations using a current first-principles theory of photoemission, and to investigate whether they were capable of reproducing the observed anisotropies. The final comparisons between theory and experiment have been presented above in Figs. 8 and 9, and have been quite successful. We now present more details of the calculations and discuss the sensitivity of the results to the various input parameters.

### A. General

The calculations, which include a full multiple-scattering treatment of the final state, are based on the reverse-scattering scheme of Zimmer and Holland.[2,18] The scattering from individual atoms was described by five phase shifts, those for Ni being derived from the Wakoh self-consistent potential,[19] while those for Na and Te were calculated using a method similar to that of Pendry[20] based on atomic wave functions tabulated by Clementi and Roetti.[21] The inelastic scattering was described by an electron damping length of 8 Å (equivalent to a mean free path of 4 Å) and the real part of the inner potential was set at 11 eV consistent with LEED studies. The structural parameters are also as determined by LEED, the adsorbate atoms sitting in the fourfold hollow at perpendicular distances of 2.23 Å for Na,[16] and 1.9 Å for Te.[17] The only parameter not taken directly from previous LEED calculation is the ratio of amplitudes of the emitted waves having $l+1$ and $l-1$ orbital character. These amplitudes are difficult to calculate reliably, but in both cases it is clear that the $l+1$ channel dominates, and as a result the azimuthal distribution is insensitive to the precise ratio of $l+1$ to $l-1$ amplitudes.

### B. Sodium

In Fig. 11 we show a comparison of our experimental results and calculations for the azimuthal variation of photoemission from the $2p$ level of Na adsorbed in the $c(2\times2)$ structure on an Ni(001) surface. The figure shows only the subtracted intensities, so no meaning can be attached to the relative intensities of the curves. Experimental data occupy the left half plane, and the theoretical calculations the right with the full curves including complete multiple scattering. Results for two different values of kinetic energy are shown. It is seen that reasonable agreement is achieved between experiment and theory, not only in the direction of the main lobes along ⟨100⟩ azimuths at 46 eV and ⟨110⟩ azimuths at 56 eV, but also in the fine details of the secondary substructure within these lobes. It is important to note that we have used no adjustable parameters.

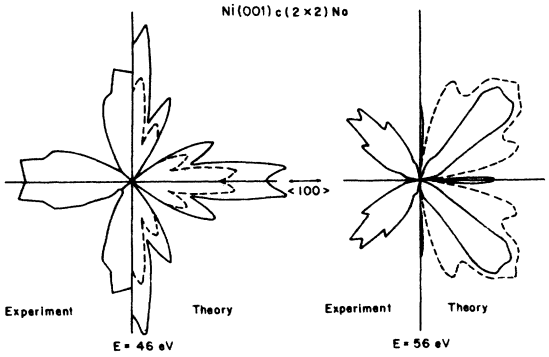


FIG. 11. Comparison between theory and experiment for the azimuthal dependence of Na $2p$ emission from Ni $(001)c(2\times2)$Na at kinetic energies of 46 and 56 eV. Only the enhanced (i.e., minimum-subtracted) results are shown, and the radial scales are arbitrary. Experimental data occupy the left half plane in each case. The calculations are shown in the right half planes, with the full curve including full adsorbate-substrate scattering and the dashed curve including adsorbate intralayer scattering only.

While this level of agreement clearly indicates that our calculations are capable of describing the structure of azimuthal anisotropies rather accurately, it is necessary to investigate the sensitivity of these patterns to changes in structure in order to determine how useful PhD may be in elucidating adsorbate structures. Some of our results appear to show little change in azimuthal pattern with quite substantial changes in adsorbate-substrate registry, and other calculations have yielded essentially identical results by ignoring scattering from the substrate entirely, indicating that adsorbate intralayer scattering dominates the azimuthal anisotropy under certain circumstances. This has led to the suggestion[22] that the azimuthal manifestation of PhD might be totally insensitive to the geometry of the substrate. In Fig. 11 we include our results (dashed curve) for the scattering from the top half monolayer of Na atoms only. At $E=46$ eV the intralayer scattering does indeed yield a pattern qualitatively indistinguishable from that for the complete system, but at the higher energy, substantial differences are evident, the large side lobes of the Na structure being absent from the full calculation and from the experimental data. At this energy therefore we expect structural sensitivity of the azimuthal distribution, and this expectation is fully realized in the calculations illustrated in Fig. 12 for the bridge, the onefold, and two fourfold structures differing in adsorbate-substrate separation. In the case of the bridge site the results of the calculations have twofold sym-

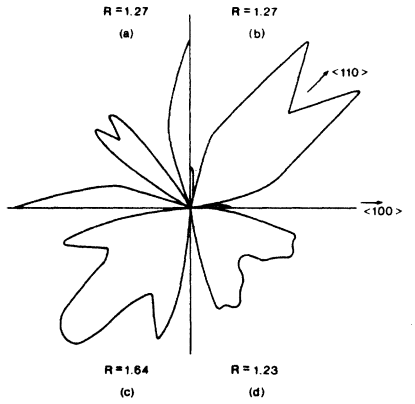


FIG. 12. Azimuthal variation of photoelectron intensity of Na $2p$ emission from Ni(001)$c(2\times2)$Na at $\theta = 30°$ and $\hbar\omega = 90$ eV for the following configurations: (a) fourfold site, $d_\perp = 2.13$ Å, (b) fourfold site, $d_\perp = 2.33$ Å, (c) bridge site, $d_\perp = 2.52$ Å, (d) onefold site, $d_\perp = 2.81$ Å. These curves have had the minimum value subtracted; the parameter $R$ corresponds to the actual maximum to minimum intensity ratios.

metry; fourfold symmetry was obtained by averaging over the two domains inevitably obtained experimentally. All four structures show dramatically different azimuthal profiles, and we note in particular the difference between Figs. 12(a) and 12(b), which show a very large change in the azimuthal pattern for a change in $d_\perp$ spacing of just 0.2 Å (i.e., from 0.1 Å below where the Na adatom is believed to lie, to 0.1 Å above this site). These model calculations demonstrate unequivocally that such patterns can be quite sensitive to surface structure.

### C. Tellurium

The comparison of theory and experiment for Te has turned out to be by no means as straightforward as for Na. We performed calculations for the azimuthal profiles at photon energies of 80, 90, and 100 eV, for a polar angle of 30° at all three energies, and additional polar angles of 45° and 60° at the lowest energy, i.e., for the data in Figs. 8 and 9. At first there was little correspondence between theory and experiment, but it was then recognized that the claculations may be very sensitive not only to structural parameters, but also to polar angle and to energy. Figure 13 gives an example of sensitivity to polar angle; for 90 eV photons the profiles at 28° and 30° are very different. Since the experimentally quoted values were accurate only to ±2°, errors in the polar angle could easily account for mutual discrepancies between experiment and theory. Figure 13 shows an extreme case of energy sensitivity; the two profiles for a photon energy of 90 eV and polar angle of 28° correspond to a difference in the real part

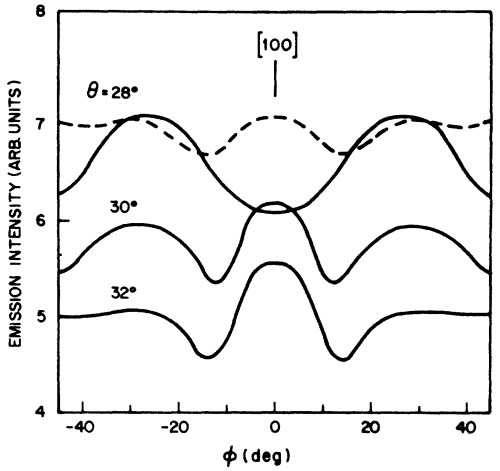


FIG. 13. Sensitivity of the azimuthal diffraction pattern to polar angle $\theta$ in the calculations for Te $4d$ emission from Ni(001)$c(2\times2)$Te. The full curves were calculated for a kinetic energy $E = 51$ eV at the polar angles $\theta$ indicated. The dashed curve was obtained at $\theta = 28°$ and $E = 53$ eV, and therefore gives an indication of the $E$ sensitivity of the calculated results.

of the inner potential of only 2 eV. Again, as with Na, we found also great sensitivity to surface structure; Fig. 14 shows the distributions at $\hbar\omega = 80$ eV and $\theta = 30°$ for $d_\perp$ spacings of 1.8, 1.9 and 2.0 Å.

In view of this sensitivity we conducted an extensive series of calculations in which the structural parameters, polar angles, and energies were varied to see if any consistent fit of the experimental data could be found. Our consistency criteria included the demand that polar angles outside the acceptable range of experimental error of ±2° should not be permitted, and further, that the inner potential was kept at 11 eV, a perhaps somewhat overly severe requirement. The only reasonable fit of the data was found for the accept-

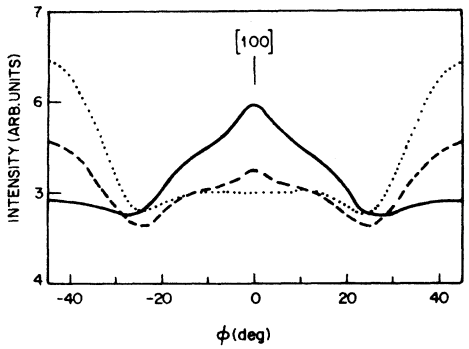


FIG. 14. Sensitivity of the azimuthal diffraction pattern to the choice of $d_\perp$ spacing in the calculations for Te $4d$ emission from Ni(001)$c(2\times2)$Te at $\theta = 30°$ and $E = 43$ eV. The full, dashed, and dotted curves correspond to $d_\perp = 1.8$, 1.9, and 2.0 Å, respectively.

ed fourfold structure with a $d_\perp$ spacing of ~1.9 Å, a variety of polar angles within the experimental error but with kinetic energies increased by 8 eV relative to the experimental values; the comparison with experiment is shown above in Figs. 8 and 9.

The question then arises as to what is the cause of this energy shift, especially as no such shift was found for the Na system. A possible explanation is the following. In the Na case the surface layer is metallic and the core hold is screened during the diffraction of the outgoing photoelectron, but in the Te case the surface is insulating and the diffraction process occurs in the presence of the Coulomb field of the core hole. If, as seems likely, the angular distribution is dominated by scattering off near neighbors of the emitter, the effective potential energy shift will be of the order of a few eV, as required.

We should remark that the effect of this energy shift is not identical to increasing the inner potential, as usually defined, to 19 eV. This would give rise to increased refraction at the surface, and in fact such calculations are found to give rather poor agreement with experiment. Rather we note that the effect of the hole will be to produce an additional spherical potential giving rise to no extra refraction; for this reason we have simulated the effect by retaining the usual 11 eV inner potential and displacing the kinetic energies in the vacuum by 8 eV. Unfortunately this remains no more than a crude simulation but a consistent treatment is beyond the scope of the theory at present. Indeed, the loss of translational symmetry which this introduces would require a radical revision of current theories.

It could reasonably be argued that the real source of our difficulties is that the representation of the photoelectron in terms of outgoing partial waves with phases determined by the neutral muffin-tin phase shifts is an inadequate description of the complicated dynamic processes that accompany photoemission. We cannot reject this criticism outright, but we note that the actual values of the phase shifts do not appear critical; for example, much the same distributions are obtained with phase shifts calculated for the potential obtained by removing an electron from the $d$ shell of Te without allowing relaxation of the electron distribution.

A useful lesson to be learned from this work on Te is that, in collecting data for a range of polar angles or energies, the increments should be small enough to allow changes in the azimuthal distributions to be followed continuously. The theory would then seek to reproduce trends in the data rather than discrete curves, which is somewhat hit-and-miss procedure in view of the great sensitivity to small changes in the parameters. It would also be desirable to perform future experiments with considerably higher angular and energy resolution than those reported here, and thereby attain the precision which the theoretical calculations indicate is possible.

## VI. CONCLUDING DISCUSSION

At the start of this project, experiments on core-level PhD had been suggested as interesting, and possibly useful, but the PhD effects had not actually been observed. Indeed there had been indications[3,23] that the backscattering amplitude, $\Psi^1$ of Eq. (1) might be too weak to bring about an observable diffraction pattern. One of our principal conclusions therefore is that, contrary to these earlier disappointments, PhD effects are readily observable and represent intensity modulations of 40% and higher. We have surveyed the various modes of observing PhD, but the bulk of our work has concentrated on the azimuthal dependence, since this is the mode which isolates the PhD effects.

Our theoretical calculations are quite encouraging and show that the existing theory of photoemission is capable of reproducing the observed diffraction patterns using the atomic structure parameters determined for LEED. In the case of Na adsorption, no adjustable parameters were required. In the case of Te adsorption, a good match between theory and experiment was achieved only by making adjustments to the stated angles and energies. Experiments at higher angular resolution should determine whether this is a serious difficulty with the theory. Most intriguing, however, was the need in the case of Te to increase the kinetic energies by 8 eV. We have speculated that this could be a real physical effect associated with the additional core-hole potential seen by outgoing photoelectron. Further work on this point could bear out the hope expressed in the Introduction that studies of the anisotropies on core-level photoemission should be helpful in arriving at a better theoretical understanding of the photoemission process itself.

Turning now to the issue of a practical surface structural technique based on PhD, the prospects are not discouraging. Comparison of the magnitudes of the observed anisotropies and the structural sensitivity tests of Sec. V suggest that $d_\perp$ spacing accuracies of ~0.1 Å should be possible. This is close to that currently attainable with LEED. As to whether PhD offers any advantages over LEED, the question remains open. Intuitively, one expects its atomic specificity to give PhD an advantage as far as density of structural information in the actual data is concerned, but fur-

ther extensive experimental and theoretical work will be required to test whether this expectation is borne out in practice. The observed similarities of the PhD data for the $p(2\times2)$ and $c(2\times2)$ configurations suggest that PhD may be more local-site sensitive and not as constrained by the need for surface periodicity as in LEED. Above all, it should be emphasized that no surface structure has yet been determined by PhD that was not already known from LEED. Workers whose prime objective is surface structure determination would not be advised by us to rush out and set up a PhD effort at this time. We observe, however, that PhD has a very attractive feature, one which it shares with the closely related new structural technique of surface-extended-x-ray-absorption fine structure[24] (SEXAFS); the experiments can be readily accomplished using rather standard photoemission spectroscopy equipment.

ACKNOWLEDGMENTS

This work was supported in part by the Science Research Council of the United Kingdom. It is a pleasure to acknowledge also the excellent help of E. M. Rowe and the staff of the University of Wisconsin Synchrotron Radiation Center (supported by the National Science Foundation under Grant No. DMR-77-21888). The monochromator was made available through the courtesy of the Science Research Council Daresbury Laboratory.

---

*Present address: Science Research Council, Daresbury Laboratory, Daresbury, Warrington WA4 4AD, United Kingdom.

[1]A. Liebsch, Phys. Rev. B 13, 544 (1976); Phys. Rev. Lett. 32, 1203 (1974).

[2]B. W. Holland, Surf. Sci. 68, 490 (1977); J. B. Pendry, Surf. Sci. 57, 679 (1976); J. W. Gadzuk, Surf. Sci. 53, 132 (1975); B. W. Holland, J. Phys. C 8, 2679 (1975).

[3]N. V. Smith, P. K. Larsen, and S. Chiang, Phys. Rev. B 16, 2699 (1977); D. Norman, D. P. Woodruff, N. V. Smith, M. M. Traum, and H. H. Farrell, Phys. Rev. B 18, 6789 (1978).

[4]D. P. Woodruff, D. Norman, B. W. Holland, N. V. Smith, H. H. Farrell, and M. M. Traum, Phys. Rev. Lett. 41, 1130 (1978).

[5]M. R. Howells, D. Norman, G. P. Williams, and J. B. West, J. Phys. B 11, 199 (1978).

[6]N. V. Smith, P. K. Larsen, and M. M. Traum, Rev. Sci. Instrum. 48, 454 (1977).

[7]H. D. Hagstrum and G. E. Becker, J. Vac. Sci. Technol. 12, 234 (1975), and private communication.

[8]S. J. White, D. P. Woodruff, and L. McDonnell, Surf. Sci. 72, 77 (1978).

[9]See, for example, D. Pines and P. Nozières, *The Theory of Quantum Fluids* (Benjamin, New York, 1960), Vol. I, p. 223.

[10]J. J. Quinn, Phys. Rev. 126, 1453 (1962).

[11]We refer here to the purely atomic effect in which the angular dependence in the emission goes as $1+\beta P_2(\cos\theta_A)$, where $\beta$ is the well-known asymmetry parameter and $\theta_A$ is the angle between $\vec{A}$ and the direction of photoelectron propagation. For further discussion, see D. Norman *et al.* in Ref. 3.

[12]S. D. Kevan, D. H. Rosenblatt, D. Denley, B.-C. Lu, and D. A. Shirley, Phys. Rev. Lett. 41, 1565 (1978).

[13]G. P. Williams, F. Cerrina, I. T. McGovern, and G. J. Lapeyre, Solid State Commun. 31, 15 (1979).

[14]C. H. Li and S. Y. Tong, Phys. Rev. Lett. 42, 901 (1979).

[15]I. T. McGovern, W. Eberhardt, and E. W. Plummer, Solid State Commun. 32, 963 (1979).

[16]S. Andersson and J. B. Pendry, Solid State Commun. 16, 563 (1975); J. E. Demuth, D. W. Jepsen, and P. M. Marcus, J. Phys. C 8, L25 (1975).

[17]J. E. Demuth, D. W. Jepsen, and P. M. Marucs, Phys. Rev. Lett. 31, 540 (1973).

[18]R. S. Zimmer and B. W. Holland, J. Phys. C 8, 2395 (1975).

[19]S. Wakoh, J. Phys. Soc. Jpn. 20, 1984 (1965).

[20]J. B. Pendry, *Low Energy Electron Diffraction* (Academic, New York, 1974).

[21]E. Clementi and C. Roetti, At. Data Nucl. Data Tables 14, 177 (1974).

[22]C. H. Li and S. Y. Tong, Phys. Rev. B 19, 1769 (1979).

[23]N. V. Smith, J. Phys. (Paris) Colloq. 39 (C4), 161 (1978).

[24]P. H. Citrin, P. Eisenberger, and R. C. Hewitt, Phys. Rev. Lett. 41, 39 (1978).